Supporting Information

for

Photo-activation and saturated emission in blended conjugated polymer nanoparticles

Xiaoli Wang[†], Louis C. Groff[†], and Jason D. McNeill*[†]

[†]Department of Chemistry, Clemson University, Clemson, SC, USA 29634

1. Calculation of dye molecule saturation intensity and saturated emission rate

The saturation intensities and saturated emission rates for Rhodamine 6G (Rh6G) and Fluorescein isothiocyanate (FITC) were calculated using the rate constants reported in the literature.[1]

The saturated excitation intensity is the excitation intensity at which the triplet state population is 50%. The population of triplet state can be expressed as,[2]

$$T_{eq} = \frac{k_{23}k_{12}}{k_{12}(k_{23}+k_{31})+k_{31}(k_{21}+k_{23})} \quad \text{(S1)}$$

where T_{eq} is the triplet population at steady-state equilibrium, and k_{12}, k_{21}, k_{23}, k_{31} represent the excitation rate, decay rate of excited singlet state, intersystem crossing rate, and decay rate of the triplet state, respectively.

The saturated emission rate is given by the following equation,[3]

$$R_\infty = \frac{1}{2}\Gamma_r \times (1+\frac{k_{23}}{k_{21}})/(1+\frac{k_{23}}{2k_{31}}) \quad \text{(S2)}$$

where R_∞ is the saturated emission rate, and Γ_r is the radiative decay rate from excited singlet state to ground state.

2. Fluorescence quantum yield determination

The fluorescence quantum yield of the CPN sample was determined with fluorescein in 0.01 M NaOH solution as standard. All the nanoparticle suspension samples and fluorescein standard were diluted to obtain absorbance of ~0.05 at 473 nm. The quantum yield of sample was calculated with the following equation and the literature value of 0.92 for fluorescein standard quantum yield.[4,5]

$$\phi_f(x) = \frac{A_s F_x n_x^2}{A_x F_s n_s^2}\phi_f(s) \quad \text{(S3)}$$

While ϕ_f is the fluorescence quantum yield, A is the absorbance at the excitation wavelength, F is the integrated area under the corrected fluorescence emission curve, and n is the solvent refractive index. Subscripts *s* and *x* represent standard and unknown sample, respectively.

3. Photobleaching curves with fitting procedures

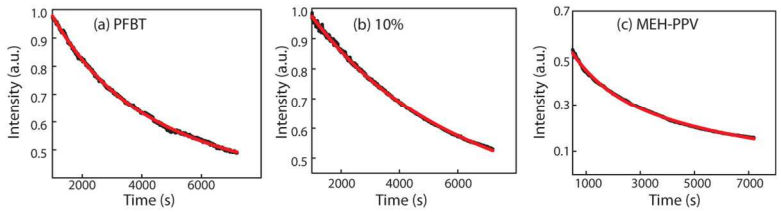

Figure S1. Photobleaching decay traces with fitting lines for (a) PFBT, (b) 10% PFBT/MEH-PPV, (c) MEH-PPV NPs.

Table S1. Fitting results for photobleaching decay traces

Sample	Starting time(s)	a_1	τ_1	a_2	τ_2	τ_{avg}	Fitting intensity at t=0 (I_0')	Real intensity at t=0 (I_0)
PFBT	1000	0.64	2600	0.56	33650	1.7×10^4	1.2	0.96
10% PFBT/MEH-PPV	1000	0.61	4160	0.51	35730	1.9×10^4	1.12	1
MEH-PPV	500	0.25	1390	0.37	8060	5.4×10^3	0.62	1

The photobleaching kinetics were complex. The photobleaching rate constants were obtained from fitting the exponential portion of the curve. For undoped PFBT nanoparticles and 10% blended nanoparticles, due to the photobrightening phenomenon at the beginning part of the trace (Figure 3(a) in the main text), we start fitting with bi-exponential decay from 1000 s. As for undoped MEH-PPV nanoparticles, there are fast decay components at the beginning part of photobleaching decay trace, ascribed to quenching by photogenerated polarons, so fitting starts from 500 s. Figure S1 shows the sample decay traces with their fitting curves, which fit well to the decay traces. Since we do not starting fitting from time 0, so there are differences between I_0' (fitting intensity at t=0) and I_0 (experimental intensity at t=0). For both PFBT and 10% blended samples, I_0' is slightly larger. For the undoped MEH-PPV sample, I_0' is much lower than I_0, which may result from the very fast decay component of MEH-PPV. The averaged photobleaching lifetime is obtained through $\tau_{avg} = (a_1\tau_1 + a_2\tau_2)/(a_1 + a_2)$.

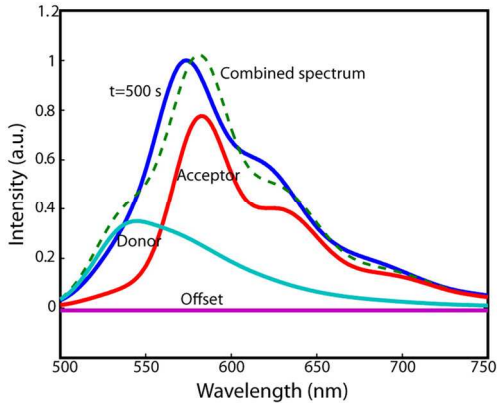

Figure S2. Decomposition of 10% blended CPNs fluorescence spectrum at photobleaching time t=500s. The original spectrum (blue), acceptor component (red), donor component (light blue), and combined spectrum (green dashed line) are shown.

In order to get a better understanding of the photobleaching behavior between acceptor and donor in the blended nanoparticle system, we decomposed the photobleaching fluorescence spectra into the donor and acceptor components. Figure S2 shows the fluorescence spectrum at photobleaching time t=500 s (blue line), acceptor MEH-PPV component spectrum (red line), donor PFBT component (light blue line), and the combined spectrum (green dashed line) by adding the donor and acceptor spectrum together. The combined spectrum approximates the real fluorescence spectrum closely.

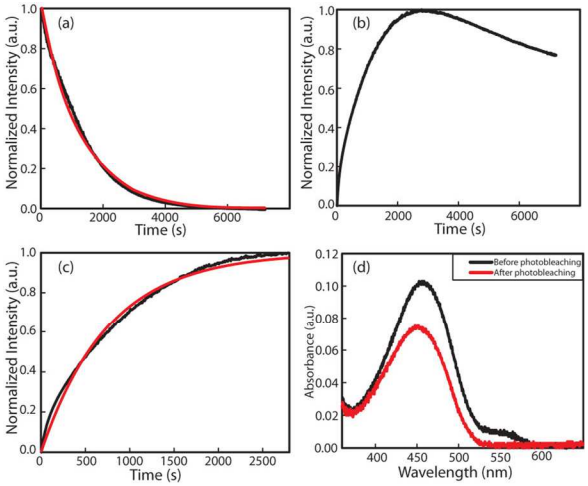

Figure S3. (a) Photobleaching trace (black) of acceptor MEH-PPV component in blended CPNs with its single exponential decay (red, $I_a = Ae^{-t/\tau}$) fit curve (red); (b) Photobleaching trace of donor PFBT in blended CPNs; (c) Photoactivation of donor PFBT emission (black) with its fit curve (red, $I_d = 1 - e^{-t/\tau}$); (d) UV-vis spectra of 10% PFBT/MEH-PPV nanoparticles before and after 2 h photobleaching.

Table S2. Fitting results

Component	Fitting function	Fitting constants	
		A	τ
MEH-PPV	$I_a = Ae^{-t/\tau}$	1.03	1260
PFBT	$I_d = 1 - e^{-t/\tau}$	--	760

The photostability for nanoparticle dispersions can be characterized by the quantum yield of photobleaching, Φ_{pb}, which is defined as the number of photobleached nanoparticles divided by the total number of photons absorbed over a given time interval, and given by the rate constant for photobleaching over the excitation rate constant. The method developed by Rigler *et al*,[6] was employed to determine photobleaching quantum yield from quantitative photobleaching kinetics measurements. The procedure detailing the photobleaching quantum yield calculation has been reported previously.[7]

4. Single nanoparticle photobleaching and saturation:

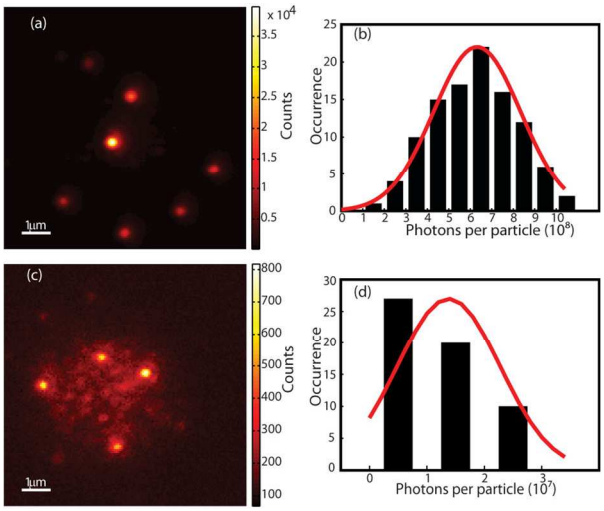

Figure S4. Representative single nanoparticle fluorescence image and emitted photon number histogram of PFBT (a, b) and MEH-PPV (c, d) nanoparticles.

The single nanoparticle photobleaching kinetics measurements were performed with the procedure provided in the main text. The single nanoparticle death numbers of the samples were determined using a custom Matlab script, taking into account the sCMOS

gain parameter and an estimated overall detection efficiency of 3% for the apparatus. The death number statistical histograms of PFBT and 10% blended samples are based on over 100 nanoparticles. For MEH-PPV, 61 nanoparticles were used.

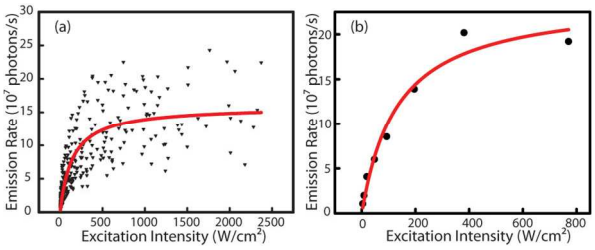

Figure S5. (a) Fluorescence saturation of single PFBT nanoparticles with increasing excitation intensity. The scattered points are the experimental data, while the solid red curve represents a fit to the saturation equation $R=R_\infty(I_e/I_s)(1+I_e/I_s)^{-1}$. (b) A single PFBT nanoparticle saturation plot with fitting.

The saturation experiments employed the typical laser intensities ranging from ~10 W/cm^2 to ~2000 W/cm^2 in the center of the laser spot to excite the sample under nitrogen protection. A series of nanoparticle mages were obtained at various excitation intensities within the given range. The excitation intensity for each single nanoparticle at sample plane was calculated based on the laser intensity at the rear epi port of the fluorescence microscope, the transmission efficiency of the objective (0.1) and the Gaussian laser excitation profile. The emission rate is the number of photons that the nanoparticle emits in one second. For the saturation plots, 30~40 nanoparticles close to the center of laser spot were analyzed.

References:

(1) Widengren, J.; Mets, U.; Rigler, R. Fluorescence Correlation Spectroscopy of Triplet-States in Solution: a Theoretical and Experimental Study. *J. Phys. Chem.* **1995**, *99*, 13368-13379.

(2) Widengren, J.; Rigler, R.; Mets, U. Triplet-State Monitoring by Fluorescence Correlation Spectroscopy. *J. Fluoresc.* **1994**, *4*, 255-258.

(3) Plakhotnik, T.; Moerner, W. E.; Palm, V.; Wild, U. P. Single-Molecule Spectroscopy-Maximum Emission Rate and Saturation Intensity. *Opt. Commun.* **1995**, *114*, 83-88.

(4) Weber, G.; Teale, F. W. J. Determination of the Absolute Quantum Yield of Fluorescent Solutions. *Trans. Faraday Soc.* **1957**, *53*, 646-655.

(5) Fery-Forgues, S.; Lavabre, D. Are Fluorescence Quantum Yields So Tricky to Measure? A Demonstration using Familiar Stationery Products. *J. Chem. Educ.* **1999**, *76*, 1260-1264.

(6) Eggeling, C.; Widengren, J.; Rigler, R.; Seidel, C. A. M. Photobleaching of Fluorescent Dyes under Conditions used for Single-Molecule Detection: Evidence of Two-Step Photolysis. *Anal. Chem.* **1998**, *70*, 2651-2659.

(7) Tian, Z. Y.; Yu, J. B.; Wang, X. L.; Groff, L. C.; Grimland, J. L.; McNeill, J. D. Conjugated Polymer Nanoparticles Incorporating Antifade Additives for Improved Brightness and Photostability. *J. Phys. Chem. B* **2013**, *117*, 4517-4520.